Scientific Research Publishing

Open Journal of Pathology, 2025, 15(4), 196-215
https://www.scirp.org/journal/ojpathology
ISSN Online: 2164-6783
ISSN Print: 2164-6775

Exacerbated Hepatic, Splenic, and Neuropathology in BALB/c Mice Co-Infected with *Leishmania major* and *Plasmodium berghei*

Richard N. Nyachieo[1,2*], Fredrick Maloba[1], Rebeccah M. Ayako[2], Jillani Ngalla[3]

[1]Department of Zoological Sciences, Kenyatta University, Nairobi, Kenya
[2]Tropical and Infectious Diseases, Kenya Institute of Primate Research, Nairobi, Kenya
[3]Non-Communicable Diseases, Kenya Institute of Primate Research, Nairobi, Kenya
Email: *richardnyakundi9@gmail.com

How to cite this paper: Nyachieo, R.N., Maloba, F., Ayako, R.M. and Ngalla, J. (2025) Exacerbated Hepatic, Splenic, and Neuropathology in BALB/c Mice Co-Infected with *Leishmania major* and *Plasmodium berghei*. *Open Journal of Pathology*, **15**, 196-215.
https://doi.org/10.4236/ojpathology.2025.154016

Received: August 13, 2025
Accepted: September 27, 2025
Published: September 30, 2025

Abstract

Co-infection with multiple protozoan parasites is a frequent yet understudied phenomenon. *Leishmania major* and *Plasmodium berghei* evoke distinct immune responses that may interact during co-infection to alter disease progression. This study aimed to evaluate the histopathological implications in BALB/c mice concurrently infected with *L. major* and *P. berghei*. One hundred sixty BALB/c mice were assigned to four groups: naïve, *L. major*-only, *P. berghei*-only, and co-infected. Body weight, parasitemia, parasite burden, and complete blood count (CBC) were monitored. Spleen and brain tissues were harvested, fixed, and examined histologically. Comparative assessments were made against naïve controls. Histopathological evaluation of BALB/c mice revealed that co-infection with *Leishmania major* and *Plasmodium berghei* induced more severe and widespread organ damage than single infections with either parasite. In the liver, co-infected mice exhibited extensive granuloma formation, diffuse infiltration of immune cells, hepatocyte degeneration, and vascular congestion. Splenic sections showed complete loss of red/white pulp boundaries, massive lymphoid follicle hypertrophy, dense leukocytic infiltration, abundant megakaryocytes, fibrosis, and pronounced hemozoin deposition. Brain tissue analysis demonstrated severe blood-brain barrier disruption, widespread hemorrhage, intense microgliosis, granuloma formation, and marked neuronal degeneration. Notably, certain neuroinflammatory and systemic pathological features—particularly extensive CNS involvement in *L. major* infection—have not been previously reported. These findings highlight the synergistic exacerbation of tissue injury in co-infection and underscore the

need for integrated control strategies in regions where leishmaniasis and malaria are co-endemic. The findings demonstrate that co-infection with *L. major* and *P. berghei* leads to exacerbated disease manifestations and altered immune homeostasis.

Keywords

Malaria, Leishmaniasis, Co-Infection, Pathology, BALB/c Mice

1. Introduction

In tropical and subtropical areas, global health is greatly impacted by parasitic diseases caused by protozoan parasites [1]. Leishmaniasis and malaria are two of the most prevalent of them affecting millions yearly. Cutaneous leishmaniasis caused by *Leishmania major* is characterized by localized skin lesions, permanent scarring and ulcerations [2] [3]. Due to its immunological parallels to human illness, several studies on *L. major* have been conducted in mouse models [4]. Contrastingly, *Plasmodium berghei* (*P. berghei*) is a rodent malaria parasite that mimics *P. falciparum*. According to [5], *P. berghei* has been a valuable model in investigating immune responses, novel antimalarial regimens and host-pathogen interactions.

Polyparasitism is rather common in endemic regions where people harbour several parasites. This has the power to drastically change the course of disease development, pathophysiology and treatment outcomes [6]. The majority of experimental models, however, examine these infections separately, perhaps ignoring intricate host-pathogen dynamics [7] [8]. Through the modulation of systemic immune responses, the erythrocyte-tropic *P. berghei* and skin-dwelling *L. major* may affect each other's replication and pathogenicity. For instance, *L. major* triggers Th1 immunity while *P. berghei* triggers both Th1 and Th2 responses [9].

To enhance diagnostic and treatment approaches, it is indispensable to understand how these disparate immune responses interrelate during co-infections. Specifically, little is known about the impact of co-infection on systemic measures that are essential for determining the severity of the disease and host tolerance, such as organ pathology. In addition to providing baseline data for creating integrated disease management strategies in co-endemic areas, this study will further our understanding of host responses to protozoan co-infections.

2. Materials and Methods

2.1. Experimental Animals

A total of 160 BALB/c mice, aged 6 - 8 weeks and weighing 18 - 22 grams, were obtained from the Animal Science Department (ASD) at the Kenya Institute of Primate Research (KIPRE), Nairobi, Kenya. BALB/c mice were selected due to their established susceptibility to L. major and compatibility with *P. berghei* infection models. Mice were housed in pathogen-free conditions, with ad libitum access to food and

water, and maintained under a 12-hour light/dark cycle at 22˚C ± 2˚C.

2.2. Experimental Parasites

2.2.1. *Leishmania major* Parasites

Leishmania major strain (MHOM/IL/81/FEBNI) was propagated in complete Schneider's Insect medium (Sigma-Aldrich Laborchemikalien GmbH, Seelze, Germany) after being aspirated from a hamster's spleen. Centrifugation at 2,500 rpm and 4˚C for 15 minutes was used to extract promastigotes at the stationary phase, as explained by [10]. After that, the pellet was centrifuged and cleaned in sterile Phosphate Buffered Saline (PBS). After that, these parasites were enumerated and 1×10^6 promastigotes were inoculated into each mouse.

2.2.2. *Plasmodium berghei* Parasites

Plasmodium berghei ANKA (wild type) cryopreserved stocks, provided by the Malaria Research and Reference Reagent Resource Center program (MR4), were recovered from liquid nitrogen and thawed at 37˚C in a water bath before being given three PBS washes at 2000 rpm for ten minutes. These parasites were then counted, and each mouse was infected with 1×10^6 infected RBCs.

2.3. Experimental Design

In this study, 160 BALB/c mice of either sex, ages 6 to 8 weeks, were obtained from the Kenya Institute of Primate Research's Rodent Facility, Animal Science Department (KIPRE [https://www.primateresearch.org/]), Karen, Nairobi, Kenya. The mice were kept in the same location for the duration of the experiment. The mice were kept in cages in a room with a temperature of 22˚C and a relative humidity of 50% - 70%. They were given mouse pellets from Unga Farm Care in Nairobi, Kenya, and they had unlimited access to water.

The BALB/c mice were split into four groups: mice infected with *L. major* only (n = 40); mice infected with *P. berghei* and *L. major* (n = 40) (co-infected with *P. berghei* 21 days after *L. major* infection); mice infected with *P. berghei* only (n = 40); and naïve mice (n = 40) (given PBS only). Intraperitoneal injections of 1×10^6 *P. berghei* and/or *L. major* parasites suspended in 100 µl of PBS were used for all infections. Spleen, liver and brain tissues were harvested on the 13th day from both experimental and control groups for histological analysis.

2.4. Histology Analysis

After the brain, liver, and spleen were harvested on the thirteenth day after infection, the organs were fixed for ten days in 10% formalin. Afterwards, they underwent the stated processing (Yamaguchi and Shen, 2013). After being dehydrated in alcohol at progressively higher percentages and decalcified in nitric acid, the tissues were submerged in xylene and embedded in melted paraffin wax. After being cut using a microtome to a thickness of 4 - 6 µm, the sections were placed on microscope slides and stained with hematoxylin-eosin stain. They were exam-

ined with a light microscope after being allowed to air dry. The slides' micrographs were taken.

3. Results

The current study investigated the impact of *Leishmania major* (a cutaneous leishmaniasis-causing protozoan), *Plasmodium berghei* (a rodent malaria parasite), and their co-infection on the pathology of mice.

3.1. Liver Pathology

Sections of the liver showed chronic inflammatory changes characterized by the formation of granulomas (yellow arrow) in the hepatic parenchyma and by massive infiltration of immune cells in hepatic sinusoids (red arrow) and portal triad (**Figure 1(A)-(B)** and **Figure 1(E)**) in the *Leishmania major* infected group. These infiltrates consisted mainly of lymphocytes (white arrows), neutrophils, and activated

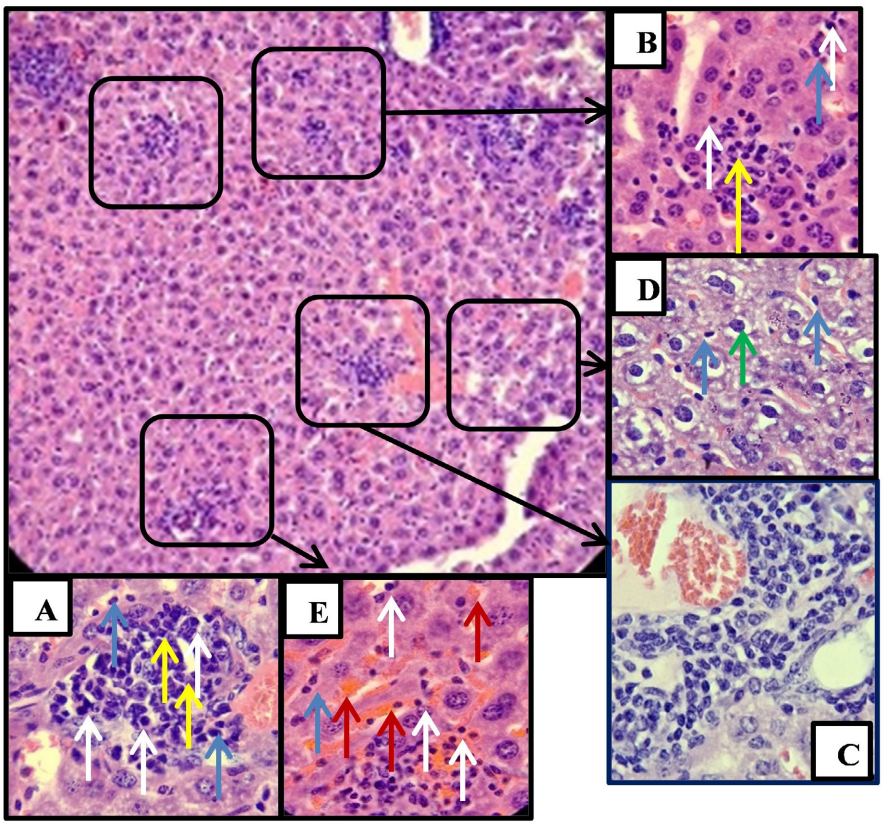

Figure 1. Histopathological analysis of *Leishmania major*-infected group liver tissue sections from BALB/c mice under different infection conditions, stained with H and E. Large box (×100) and smaller boxes (×1000). (A) Severe inflammation, proliferation, and infiltration of Kupffer cells (blue arrow) within the hepatic structure, resulting in granuloma formation (yellow arrow). (B) Granuloma formation—aggregates of Kupffer cells and mononucleated immune cells (white arrow). (C) perivascular cuffing—aggregates of mixed immune cells infiltration Kupffer cells (blue arrow) around congested hepatic vessels (red arrow). (D) Degeneration of hepatocytes—hepatocyte nucleus atypia, pyknosis, cytoplasmic loss and vacuolation (green arrow). (E) Hepatocyte sinusoids vasodilation and congestion (red arrow).

The lobular liver architecture was highly destroyed in the mice with *Plasmodium berghei* infection. Typical was the presence of hemozoin pigment (orange arrow, Figure 2(E)) (brown to black granules) accumulating, mainly within hepatic vessels and sinusoids in association with phagocytic Kupffer cells (blue arrows) (Figure 2(A), Figure 2(B) and Figure 2(D)) Granulomas (yellow arrows) were present but smaller and less mature than in the *Leishmania*-only group (Figure 2(A), Figure 2(D) and Figure 2(F)). The degeneration of hepatocytes had occurred with pyknosis, karyolysis, and hepatocyte hypertrophy. Increased congestion of hepatic vasculature together with increased sinusoids indicated a defective hepatic blood flow. The prevalent inflammatory infiltrate spread through the hepatic sinusoids (red arrows) veins and portal triads, and reflected active immune stimulation systemically (Figure 2(C), Figure 2(D) and Figure 2(F)).

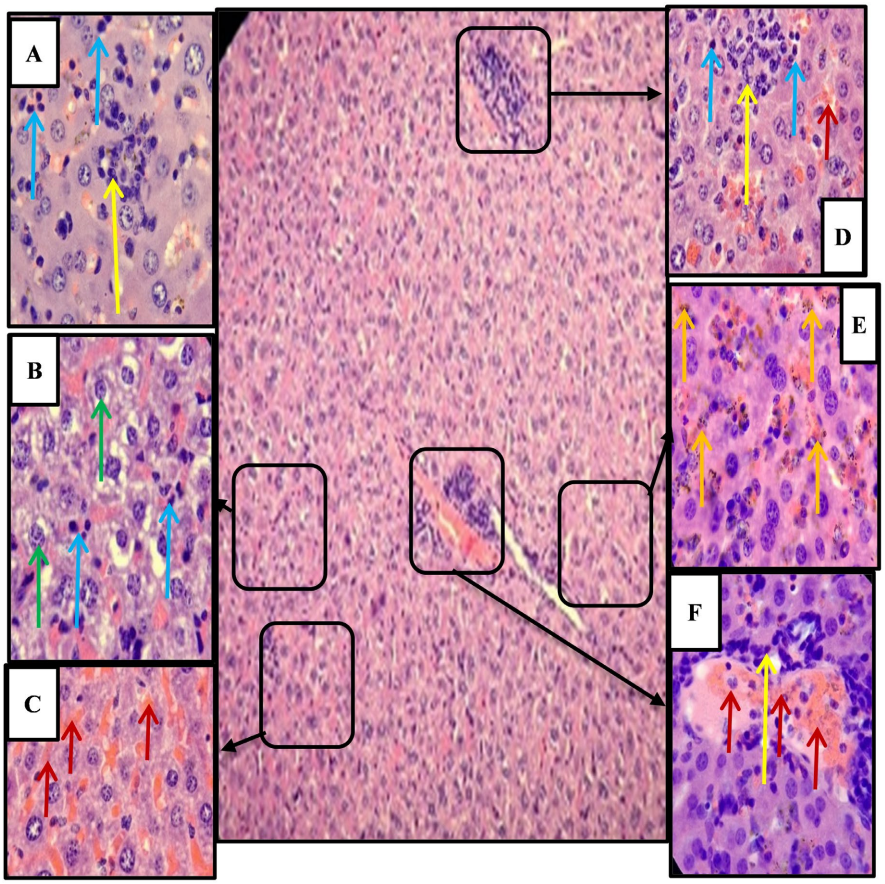

Figure 2. Histopathological analysis of *Plasmodium berghei*-infected group liver tissue sections from BALB/c mice under different infection conditions, stained with H and E. Large box (×100) and smaller boxes (×1000). (A) Granuloma (yellow arrow) formation with moderate infiltration of Kupffer cells (blue arrow). (B) Degeneration of hepatocytes (green arrow)—nucleus atypia, pyknosis, cytoplasm loss and microvacuolation. (C) Hepatic sinusoids vasodilation and congestion (red arrow). (D) Moderate immune cell infiltration with granuloma formation (yellow arrow) characterized by hypertrophied Kupffer cells infiltration (blue arrow) and hepatic sinusoid congestion (red arrow). (E) Extensive hemozoin deposition (brown to black pigments) within the hepatic parenchyma (orange arrow).

Histopathological changes became severe in co-infected mice and showed an overlapping impact of the two infections. Granulomas had proliferated with diffuse infiltrate by the immune cells within sinusoids (red arrow, Figure 3(A) and Figure 3(E)), portal triad and liver vein (orange arrow) (Figure 3(B)). Usually Kupffer cells were hypertrophied, and some were seen to be parasitized (blue arrow, Figure 3(A) and Figure 3(C)) and this indicated phagocytic activity was present. Hepatic degeneration was seen in a patchy manner with karyolysis, pyknosis and vacuolent changes in the hepatocytes (black arrow, Figure 3(D)). Surprisingly, there was a smaller granuloma and diminished immune infiltration during later infection stages and this could be a marker of immunomodulatory interactions (yellow arrow, Figure 3(E)). It also had a considerable degree of vascular congestion but presence of hemozoin pigment was present though less evident when compared with the malaria-only group.

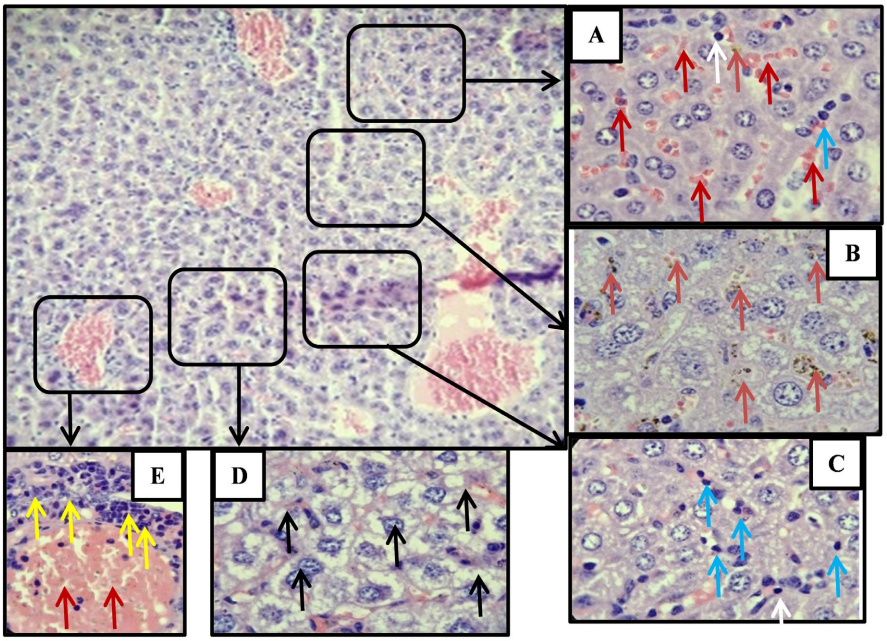

Figure 3. Histopathological analysis of *Leishmania major-Plasmodium berghei* co-infected group liver tissue sections from BALB/c mice under different infection conditions, stained with H and E. Large box (×1000) and smaller boxes (×400). (A) Vasodilation and congestion of the hepatic sinusoids (red arrow). (B) Extensive coarse hemozoin (brown to black pigments) deposition within the hepatic sinusoids (orange arrow). (C) Moderate immune cell infiltration (Kupffer cells) within the hepatic parenchyma (blue arrow). (D) Degeneration of hepatocytes- atypia of the hepatocyte nucleus, cytoplasmic loss and vacuolation (clear space surrounding the nucleus, black arrow). (E) immune cell aggregates surrounding the vascular system (perivascular cuffing)/granuloma formation (yellow arrow), congestion of the hepatic vessels.

Liver tissues from naïve (uninfected) mice (Figure 4) demonstrated preserved hepatic architecture, with intact lobular organization, absence of inflammation, degeneration, or vascular congestion—serving as a healthy baseline reference.

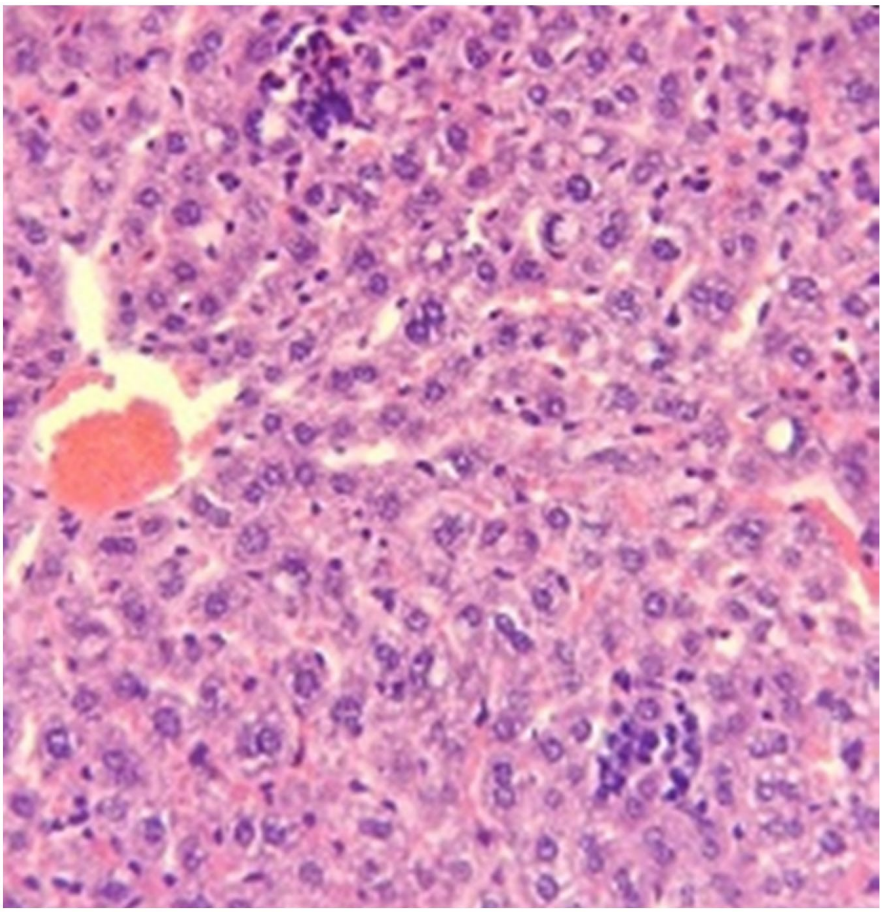

Figure 4. Histopathological analysis of liver tissue sections from BALB/c mice under different infection conditions, stained with H and E (1000× magnification). Intact hepatocyte cells with a normal hepatocyte nucleus and Kupffer cells infiltration.

3.2. Spleen Pathology

Accounting by sections of the spleen in *Leishmania major*-infected mice showed a highly anomalous structure in all histological surveys. The boundary between the red and white pulp was delineated poorly and there was evidence of disordered (blue arrow, **Figure 5(A)** and **Figure 5(E)**), enlarged lymphoid follicles that in many cases protruded into the red pulp. Numerous these follicles were vacuolated and degenerating in germinal centers. Immune cells with mononucleated and multilobed leukocytes were highly infiltrated into the red pulp, which indicated an increased level of inflammatory response (white arrow, **Figure 5(A)**, **Figure 5(B)** and **Figure 5(D)**). Evidence of extramedullary hematopoiesis was also evident by the occasional presence of megakaryocytes (yellow arrows, **Figure 5(B)** and **Figure 5(C)**) within the parenchyma, probably a compensatory effect of well-documented systemic effects such as anemia. Chronic inflammation was associated with fibrosis, in which collagen deposition (green arrows, **Figure 5(D)**) and fibroblast infiltration were apparent within white and red pulp areas (black arrow, **Figure 5(A)** and **Figure 5(E)**). Also, there was an increase in overall cellularity and moderate amounts of hemozoin pigment deposits were evident, which could

be attributed to either increased macrophage activity or leftover starting baseline pigment (orange arrow, Figure 5(C)).

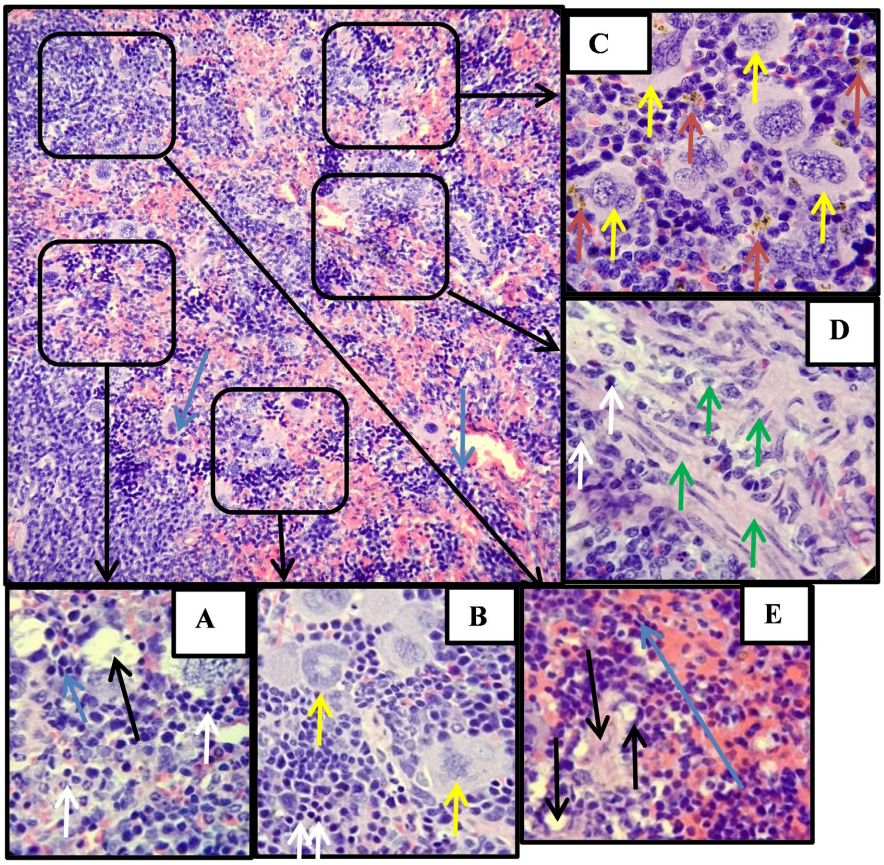

Figure 5. Histological evaluation of splenic architecture in *Leishmania major* infected BALB/c mice under different infection conditions, stained with H and E. Large box (×100) and smaller boxes (×1000). (A) Disorganization of the splenic architecture with the white pulp (lymphoid follicles) scattered into the red pulp (blue arrow). (B) Severe inflammation with Immune cell infiltration- proliferation of mononucleated leucocytes (white arrow). (C) Numerous megakaryocytes (yellow arrows), moderate hemozoin deposition (orange arrows). (D) Collagen deposition and fibroblast infiltration-fibrosis (green arrow). (E) Degeneration of germinal centers-vacuolation, fibrin deposits (black arrows).

Architectural distortion was also profound in the spleens of *P. berghei*-infected mice. There was a disruption of the marginal zone, and the white pulp had been hypertrophic with enlarged germinal centers suggesting a significant degree of B-cell activation (yellow arrows, Figure 6(E)). There were also degenerative alterations like vacuolation. There was a robust immune infiltrate of the red pulp comprising not only lymphocytes and neutrophils (black and white arrows, Figure 6(A), Figure 6(C) and Figure 6(E)) but also widespread megakaryocyte infiltration (blue arrows) indicative of reactive extramedullary hematopoiesis (Figure 6(B)), Figure 6(D) and Figure 6(E)). Typically during malaria pathology, hemozoin deposits were intense all over the splenic parenchyma (orange, Figure 6(C) and Figure 6(D). The vascular sinusoids (red arrows Figure 6(C) and Figure 6(D))

were remarkably dilated, which signifies congestion and fibrotic changes with presence of collagens and fibroblasts an indication of continued tissue remodeling caused by tissue inflammation. There were immune aggregates and hypercellularity indicative of intense immune activation.

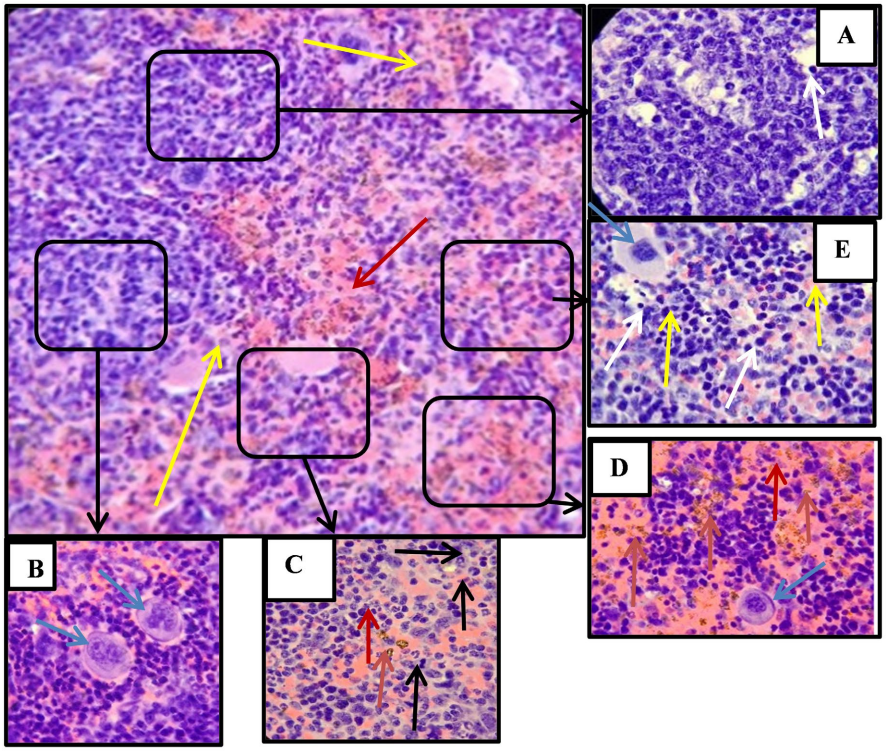

Figure 6. Histological evaluation of splenic architecture in *Plasmodium berghei* infected BALB/c mice under different infection conditions, stained with H and E. Large box (×100) and smaller boxes (×1000). (A) Splenic architecture changes, including blurring of the marginal zone and hypertrophy of the germinal centres. Follicles in the red pulp (yellow arrow). (B) Numerous megakaryocytes infiltration within splenic parenchyma (blue arrow). (C) and (D) Vasodilation of splenic vascular sinusoids/spaces and congestion (red arrows) and extensive coarse hemozoin deposits—brown to black pigments in the red pulp (orange arrow). Cand (E) Severe inflammation with immune cells infiltration (mononucleated leucocytes—white arrow) and multilobed leucocytes—black arrow).

The splenic structure was the worst affected in the co-infected mice. There was a total loss of distinction between the red and the white pulp, the white pulp showing extensive loss of organization, hypertrophy and infiltration with lymphoid follicles into red pulp (yellow arrows, **Figure 7(A)** and **Figure 7(C)**). Degeneration was found in both pulp regions, manifesting itself in the form of cell lysis and vacuolation (green arrow, **Figure 7(D)**), which points to the high level of cellular stress. There was excessive extramedullary erythropoiesis with megakaryocytes being heavily infiltrated all over the spleen (blue arrow, **Figure 7(B)** and **Figure 7(E)**). Severe inflammatory activity was demonstrated by intense immune cells infiltration in the form of dense leukocytic clusters, as well as mononuclear/multilobed

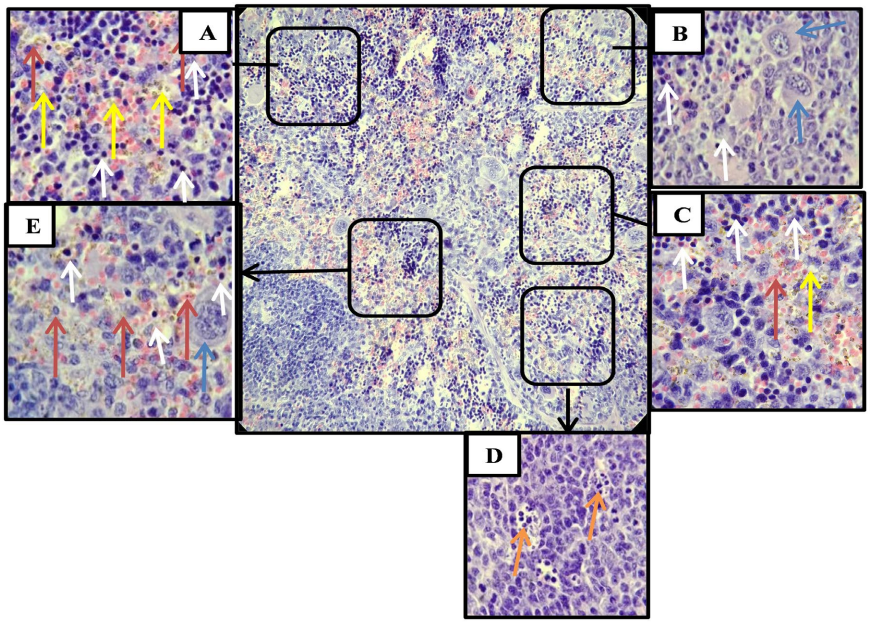

Figure 7. Histological evaluation of splenic architecture in *Leishmania major-Plasmodium berghei* co-infected BALB/c mice under different infection conditions, stained with H and E. Large box (×100) and smaller boxes (×1000). (A) Hypertrophy of white pulp—germinal center with reactive follicle infiltration into red pulp with vacuolation and loss of the marginal zone (yellow arrow). (B) Numerous megakaryocytes infiltration in the red pulp and white pulp (blue arrow). (C) Severe inflammation—Immune cell infiltration (mononucleated leucocytes)—white arrow. (D) Degeneration of the spleen white and red pulp with blurry marginal zone and vacuolation of the germinal center (green arrow). (E) Extensive coarse hemozoin deposition within the white and red pulp (orange arrows).

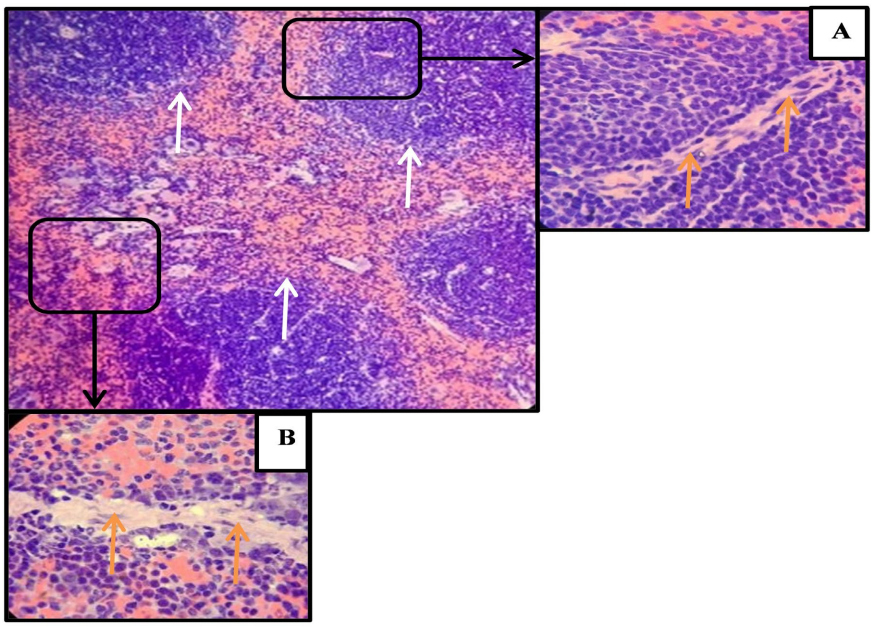

Figure 8. Histological evaluation of splenic architecture in naïve BALB/c mice under different infection conditions, stained with H and E. Large box (×100) and smaller boxes (×1000). (A) Well outline and demarcation of the white and red pulp (white arrow). (B) Well-organized connective tissue (trabeculae) (green arrow).

leukocytes, (white arrows, Figure 7(A)-(C) and Figure 7(E)). As shown by the hemozoin deposits (orange arrows, Figure 7(A), Figure 7(C) and Figure 7(E)), there was malaria pathology, with collagen and fibroblast infiltration indicating chronicity and tissue-repair response that had been initiated.

In contrast, spleens from naïve (uninfected) mice exhibited intact architecture, with well-demarcated red and white pulp (Figure 8(A)), and no signs of inflammation, degeneration, or fibrosis (Figure 8(B)), serving as a baseline for comparison.

3.3. Brain Pathology

Brain histopathological analysis of *Leishmania major* infected mice showed that the architecture of the brain was slightly distorted. Microscopic alterations exhibited notable findings which were mild accumulation of fibrous tissue in the parenchyma (green arrow, Figure 9(F)), disruption of Blood-Brain Barrier (BBB) in form of hemorrhage and extravasated red blood cells (red arrow, Figure 9(A), Figure 9(D) and Figure 9(E)), and presence of immune cells, especially activated microglia (blue arrow, Figure 9(A)-(C) and Figure 9(D)). Such changes correlated with granuloma and glial proliferation. Some of the changes in the neurons were pyknosis (black arrow, Figure 9(D)), vacuolation (yellow arrows, Figure 9(E)), and hypertrophy of pyramidal neurons and granular cells, which had hyperchromatic aggregates as well as degenerative characteristics like nuclear lysis and formation of pericellular spaces.

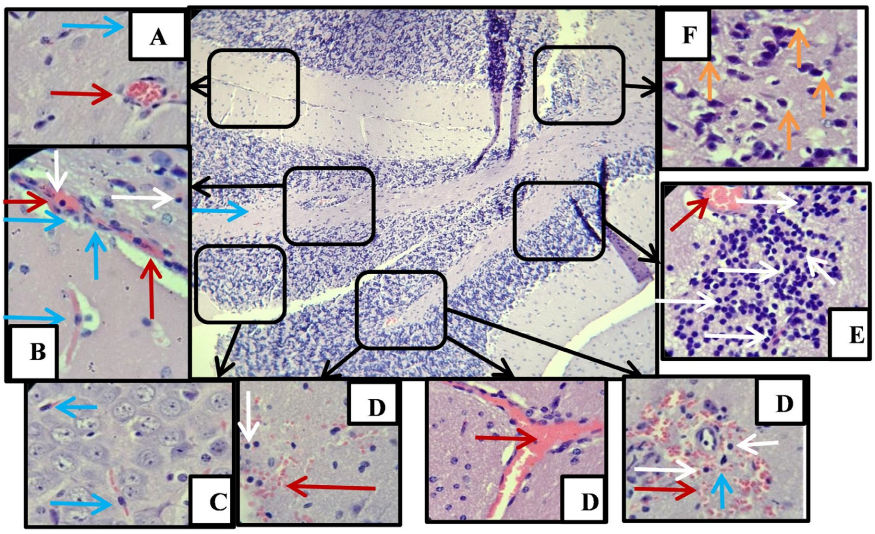

Figure 9. Histopathological assessment of brain tissue from *Leishmania major*-infected BALB/c mice under different infection conditions, stained with H & E. Large box (×100) and smaller boxes (×1000). (A) Hemozoin deposits and extravasated red blood cells (red arrow), mononucleated immune cells (white arrow), microglia cells infiltration (blue arrow) and blood-brain barrier disruption. (B) Microglia infiltration (blue arrow). (C) granular cell layer degeneration-hypochromasia of granular cells, development of a clear halo space surrounding the nucleus and vacuolation (green arrow). (D) Degeneration of the pyramidal cells-pyramidal cell nucleus pyknosis, presence of a clear space around the nucleus-vacuolation (black arrow). (E) Degeneration of Purkinje cells and cell layer-Purkinje cell lysis and vacuolation (yellow arrows).

There was greater neuropathology in mice that were infected with *Plasmodium berghei*. The BBB was extremely disrupted with clogged blood vessels (red arrow, Figure 10(C)-(E)) in the parenchyma and the massive vascular congestion. Mononuclear cells infiltrated the perivascular space (blue arrow, Figure 10(C)-(E)) and microglia were densely activated (blue arrow, Figure 10(B)). The brain microvasculature contained malaria parasite-infected cells in hemoglobin and hemozoin pigment and immune cell infiltration of the brain tissue. There was massive destruction of the Purkinje cells, where their pyknosis, vacuolation and cell lysis were seen (green arrows, Figure 10(A)) and there were also pyramidal and granular degenerative changes in the pyramidal and granular neurons (Figure 10(A)).

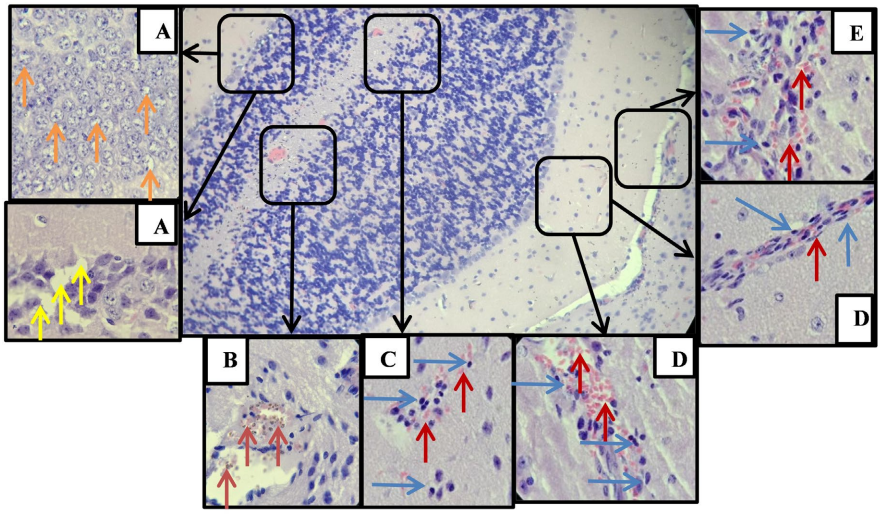

Figure 10. Histopathological assessment of brain tissue from *Plasmodium berghei*-infected BALB/c mice under different infection conditions, stained with H & E. Large box (×100) and smaller boxes (×1000). (A) Congestion of the brain microvasculature. (red arrow). (B) congestion of the brain microvasculature red arrow) and microglial cells infiltration within the brain vessels (blue arrow). (C) and D) Extravasation of the red blood cells within the brain tissue with mild mononucleated immune cell infiltration (white arrow). (E) Aggregates of mononucleated immune cells infiltration within the brain tissue (white arrow). (F) Degeneration of the pyramidal cells with nucleus pyknosis and microvacuolation with a clear space surrounding the pyramidal cell nucleus (green arrow).

The most severe pathological changes in co-infected mice were vast hemorrhage, breakdown of the BBB, infiltration of RBC (red arrow, Figure 11(A)) with a significant invasion of the mononucleated leukocytes (white arrow, Figure 11(A)) and dense microglial infiltration (blue arrow, Figure 11(B)). Major distortion of brain architecture was caused by severity of proliferating glia and the formation of granulomas. Degeneration of neurons was widespread, involving the Purkinje, granular and pyramidal cell layers with a meager hypochromatic cytoplasm, shrinkage, karyolysis and vacuolation (cyan and black arrows, Figure 11(B)-(D)). Presence of deposits of hemozoin (orange arrows, Figure 11(A)) also reaffirmed the active malaria exposure, questioning a combined inflammatory and degenerative effect because of co-infection.

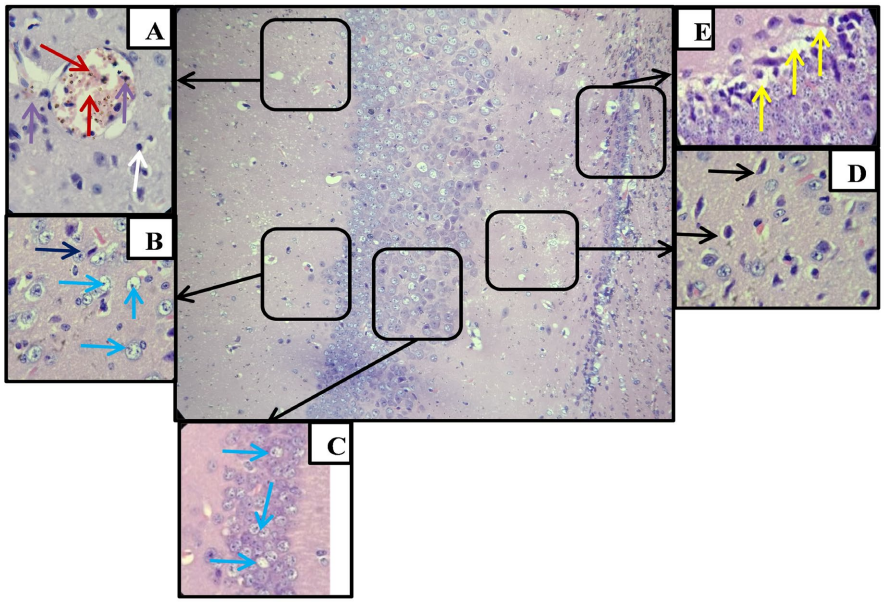

Figure 11. Histopathological assessment of brain tissue from *Leishmania major-Plasmodium berghei* infected BALB/c mice under different infection conditions, stained with H and E. Large box (×100) and smaller boxes (×1000). (A) Hemozoin deposits (orange arrow), extravasated red blood cells (red arrow), mononucleated immune cells (white arrow), microglia cells infiltration (blue arrow) and blood-brain barrier disruption. (B) Microglia infiltration (blue arrow). (C) granular cell layer degeneration- hypochromasia of granular cells, development of clear halo space surrounding the nucleus and vacuolation (cyan arrow). (D) Degeneration of the pyramidal cells-pyramidal cell nucleus pyknosis, presence of a clear space around the nucleus-vacuolation (black arrow). (E) Degeneration of Purkinje cells and cell layer—Purkinje cell lysis and vacuolation (yellow arrows).

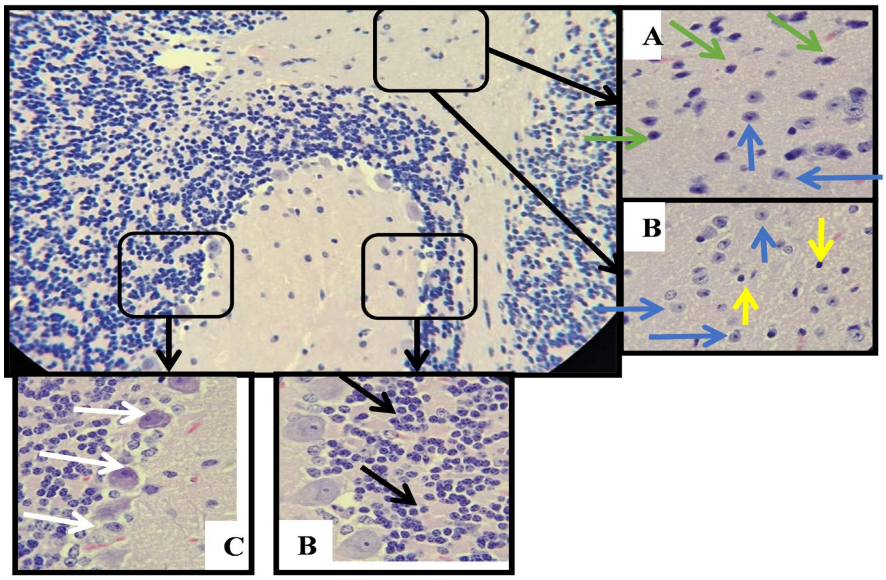

Figure 12. Histopathological assessment of brain tissue from naïve BALB/c mice under different infection conditions, stained with H & E. Large box (×100) and smaller boxes (×1000). (A) Normal nerve cells (blue arrow), oligodendrocytes (yellow arrows), and normal pyramidal cells (green arrow). Normal cerebellar cortex. (B) Normal granular cells/layer (black arrow). (C) Normal Purkinje cells/layer (white arrow).

Naïve (uninfected) control mice displayed normal brain architecture, with no evidence of hemorrhage, inflammation, or neuronal degeneration {blue (**Figure 12(A)** and **Figure 12(B)**), yellow (**Figure 12(B)**), green (**Figure 12(A)**), black (**Figure 12(B)**) and white (**Figure 12(C)**) arrows. This preserved structure provided a reference for the pathological features observed in the infected groups.

4. Discussion

The granuloma formation observed in the liver, spleen and brain tissues in the *Leishmania major*-infected group aligns with prior studies demonstrating hepatic granulomatous responses in visceral and cutaneous leishmaniasis, even in non-visceral strains, due to hepatic parasite migration or antigen deposition [11]-[13]. Similar studies using *Leishmania donovani* in mice and hamsters have documented granulomas composed of mononuclear cells, especially Kupffer cells, with concurrent hepatocyte damage and fibrosis [12].

The liver pathology seen in *P. berghei*-infected mice is consistent with findings from malaria studies in rodent models. Hemozoin accumulation within Kupffer cells and sinusoids, hepatic congestion, and hepatocyte degeneration are hallmark features reported in both *P. berghei* and *P. chabaudi* infections [14] [15]. These changes are associated with systemic inflammation, hypoxia, and the hepatocellular stress response triggered by parasitized red blood cells and inflammatory cytokines.

Interestingly, the co-infection model showed histological features of both pathogens but with potentially moderated responses. For instance, while immune infiltration and hepatocyte damage were severe, granuloma formation and hemozoin deposition appeared less pronounced than in single infections. This suggests an immunological interaction where *L. major* infection may alter the hepatic microenvironment or modulate the host immune response to *P. berghei*, reducing pigment accumulation and fibrotic changes. Comparable immunomodulatory effects have been described in co-infection studies, such as *Leishmania-Trypanosoma* or *Leishmania-Plasmodium* models, where altered cytokine profiles and macrophage activation states impact pathology [3] [9].

The observation that *L. major* co-infection appeared to reduce cerebral hemozoin deposition in P. berghei-infected mice suggests that the dermotropic parasite may alter host immune dynamics in a way that modifies malaria pathogenesis. One potential mechanism involves macrophage activation states. *L. major* infection drives strong macrophage responses that can skew toward either a classical (M1) or alternative (M2) phenotype depending on host genetics and cytokine milieu [16] [17]. An M1-skewed response, enriched in IFN-γ, TNF-α, and nitric oxide, could enhance phagocytic clearance and degradation of parasitized erythrocytes, thereby limiting hemozoin accumulation [9]. Conversely, M2-associated cytokines such as IL-4 and IL-10 might dampen the excessive inflammatory activation that typically fuels malaria-associated pathology, thus modifying hemozoin deposition indirectly [18].

Similarly, cytokine cross-regulation between the two infections may contribute. *Leishmania major* infection is known to induce strong Th1-associated cytokines (IL-12, IFN-γ) in resistant strains or Th2-associated cytokines (IL-4, IL-10) in susceptible strains [19] [20]. In the context of *P. berghei* co-infection, a Th1-dominant profile could improve parasite control and erythrocyte clearance efficiency, while IL-10 production could restrain hyperinflammation and reduce monocyte-driven hemozoin accumulation in cerebral microvessels [21]. Furthermore, chemokines such as CCL2 and CXCL10, upregulated during leishmanial infection, may alter leukocyte trafficking into the brain and change the cellular niche where hemozoin is deposited.

In *L. major*-infected mice, the disruption of splenic architecture, particularly the blurring of the marginal zone and hypertrophy of lymphoid follicles, reflects an active humoral immune response. Such disorganization is consistent with prior observations in *Leishmania* donovani infections, where splenic white pulp disintegration and follicular atrophy are linked to chronic antigenic stimulation [16]. Though *L. major* is typically considered dermotropic, this study reinforces the systemic immunopathological impact it can exert during sustained infection.

The presence of megakaryocytes and fibrotic changes signifies extramedullary hematopoiesis and chronic inflammation, respectively. Similar findings [17] noted increased megakaryocyte activity in the spleens of mice infected with *Leishmania*, possibly reflecting a host response to anemia or bone marrow suppression. The observed collagen deposition and fibroblast infiltration align with studies showing that chronic leishmaniasis induces stromal remodeling in lymphoid organs [9] [18].

Interestingly, the detection of hemozoin pigment in *L. major*-infected spleens, albeit moderate, may suggest macrophage activation or prior immune priming. While hemozoin is typically a byproduct of hemoglobin digestion by malaria parasites, reports such as [19] [20] indicate that macrophages in leishmaniasis can sequester pigment remnants from previous co-infections or systemic inflammation. The splenic pathology in *P. berghei*-infected mice is characterized by white pulp hypertrophy, germinal center enlargement, and significant red pulp infiltration. These features are hallmark responses to malaria-induced hyperactivation of the immune system. [20] reported similar germinal center changes in murine models of cerebral malaria, attributing them to robust B-cell responses and cytokine storms.

Prominent hemozoin accumulation, a well-established malaria pathology marker, was widely distributed in the splenic tissue in our study. This finding is in line with prior studies [21] [22] that describe hemozoin as both a diagnostic marker and an immunomodulatory agent contributing to systemic inflammation. The fibrotic changes and sinusoidal dilation observed here suggest tissue adaptation to prolonged immune activation and vascular stress, confirming findings [23] on chronic splenic damage in *Plasmodium*-infected rodents. Megakaryocyte infiltration again supports the presence of reactive extramedullary hematopoiesis a phe-

nomenon documented in severe and chronic malaria as a response to anemia and bone marrow suppression [15].

The co-infected group exhibited the most profound architectural disruption and immune dysregulation, with total obliteration of red/white pulp boundaries, excessive lymphoid follicle expansion, and intense immune cell infiltration. These results illustrate an additive or synergistic pathological impact, consistent with the hypothesis that polyparasitic infections exacerbate host tissue damage. The combined presence of degenerative features (e.g., vacuolation, cell lysis), high-density immune clusters, abundant megakaryocytes, and fibrotic remodeling is suggestive of overwhelming immune stimulation and chronic inflammation. Studies support the view that co-infections can dysregulate immune homeostasis, leading to both overactivation and exhaustion [3] [24].

Furthermore, the enhanced hemozoin burden and fibroblast infiltration indicate both active malaria pathology and long-standing tissue damage and repair processes, respectively. These findings underscore the complex interplay between immune responses to different parasites and the resulting structural compromises in lymphoid organs. The mild disruption in brain architecture observed in *L. major*-infected mice, including fibrous deposition, immune infiltration, and granuloma formation, aligns with earlier reports indicating that while *L. major* is primarily dermotropic, it can induce neuroinflammatory changes under certain conditions. [25] reported microglial activation and glial proliferation in the cerebral cortex of *Leishmania donovani*-infected rodents, which is consistent with the activated microglia and gliosis noted in our study. However, our data suggest that even in cutaneous leishmaniasis, such as with *L. major*, systemic inflammatory responses may extend into the Central Nervous System (CNS), albeit to a milder degree compared to visceralizing species.

The mild disruption of brain architecture in *Leishmania major* infected mice characterized by fibrous deposition, immune cell infiltration, granuloma-like foci, and accompanying microglial activation with gliosis supports the emerging view that Cutaneous Leishmaniasis (CL), despite its predominantly dermotropic tropism, can exert measurable effects on the Central Nervous System (CNS) under specific inflammatory milieus. Prior studies in Visceral Leishmaniasis (VL), especially with *L. donovani*, have documented microglial activation, glial proliferation, and perivascular inflammatory changes in rodent models; your findings are concordant with this neuroinflammatory signature but scaled down in magnitude, consistent with the lower systemic parasite burden and tissue dissemination typical of *L. major* relative to visceralizing species.

Furthermore, the neuronal alterations observed, such as pyknosis, vacuolation, and nuclear lysis are similar to those seen in chronic neuroinflammatory conditions and suggest potential neurotoxic effects mediated by cytokines or parasite-derived molecules. This aligns with [26], which demonstrated that cytokine storms induced by chronic Leishmania infection can cause neural stress and cellular damage in peripheral and central nervous tissues. Our findings in *P. berghei*-infected

mice revealed hallmark features of cerebral malaria, including widespread BBB breakdown, perivascular leukocyte infiltration, and deposition of hemozoin. These results are in agreement with previously documented cerebral pathology in murine models of cerebral malaria (SCM). [27] [28] described severe vascular pathology and widespread neurodegeneration in *P. berghei* ANKA-infected C57BL/6 mice, with extensive microglial activation and parasite sequestration in brain capillaries findings that mirrored our observations of microglial clustering and hemozoin-laden vessels.

The co-infected mice demonstrated exacerbated neuropathology, surpassing the severity seen in single infections. This synergistic effect supports the hypothesis that co-infections can exacerbate inflammatory and neurodegenerative processes. Previous studies examining co-infection effects have shown that concurrent parasitic infections can heighten systemic immune activation, leading to more pronounced tissue damage [29] [30]. Notably, the compounded effects on BBB integrity, immune infiltration, and neuronal loss in our study suggest that co-infection intensifies CNS pathology via both immune-mediated mechanisms and direct parasitic insults. Hemozoin deposits, extensive microgliosis, and severe glial proliferation in co-infected mice provide compelling evidence of an additive or possibly synergistic neuropathogenic interaction between *Leishmania* and *Plasmodium*.

Co-infection with *Leishmania major* and *Plasmodium berghei* caused more severe tissue damage than either infection alone. In the liver, mice showed extensive granuloma proliferation, immune cell infiltration, hepatocyte degeneration, and vascular congestion. Spleens showed disruption of red/white pulp boundaries, leukocytic infiltration, and fibrosis. Brain sections showed severe blood-brain barrier disruption, hemorrhage, and neuronal degeneration. Future studies should investigate immunological interactions driving synergistic tissue damage. Histological descriptions of fibrous deposition, microglial activation, and granuloma formation provide qualitative evidence, but without detailed quantitative morphometry, immunohistochemistry, or imaging, subtle differences may be under- or over-estimated.

Acknowledgements

We would like to acknowledge Dr. Benjamin Mwongela, Mr. Kenneth Waititu, Mr. Thomas Adino, Mrs. Priscilla Kimiti, Ms. Gladys Korir and Mr. Dominic Mwaura from the Animal Science Department, KIPRE, without whom this study would not have been a success.

Ethical Approval

Approval for the project was sought from the Institutional Scientific and Ethical Review Committee (ISERC) of the Kenya Institute of Primate Research (KIPRE) (study ISERC/10/2016). Animal experiments were recognized under great care and the protocols were conformed under the Institutional Animal Care and Use

Committee (IACUC) and included the internationally accepted standards of conducting animal researches. There were humane endpoints in the course of the study to reduce suffering in animals.

Conflicts of Interest

The authors declare no conflict of interest.

References

[1] Kaminsky, R. and Mäser, P. (2025) Global Impact of Parasitic Infections and the Importance of Parasite Control. *Frontiers in Parasitology*, **4**, Article 1546195. https://doi.org/10.3389/fpara.2025.1546195

[2] Oryan, A. and Akbari, M. (2016) Worldwide Risk Factors in Leishmaniasis. *Asian Pacific Journal of Tropical Medicine*, **9**, 925-932. https://doi.org/10.1016/j.apjtm.2016.06.021

[3] Pinna, R.A., Silva-dos-Santos, D., Perce-da-Silva, D.S., Oliveira-Ferreira, J., Villa-Verde, D.M.S., De Luca, P.M., *et al*. (2016) Malaria-Cutaneous Leishmaniasis Co-Infection: Influence on Disease Outcomes and Immune Response. *Frontiers in Microbiology*, **7**, Article 982. https://doi.org/10.3389/fmicb.2016.00982

[4] Torres-Guerrero, E., Quintanilla-Cedillo, M.R., Ruiz-Esmenjaud, J. and Arenas, R. (2017) Leishmaniasis: A Review. *F1000Research*, **6**, Article 750. https://doi.org/10.12688/f1000research.11120.1

[5] Otun, O. and Achilonu, I. (2025) *Plasmodium yoelii* as a Model for Malaria: Insights into Pathogenesis, Drug Resistance, and Vaccine Development. *Molecular Biology Reports*, **52**, Article No. 208. https://doi.org/10.1007/s11033-025-10318-4

[6] Leitner, W.W., Bergmann-Leitner, E.S. and Angov, E. (2010) Comparison of *Plasmodium berghei* Challenge Models for the Evaluation of Pre-Erythrocytic Malaria Vaccines and Their Effect on Perceived Vaccine Efficacy. *Malaria Journal*, **9**, Article No. 145. https://doi.org/10.1186/1475-2875-9-145

[7] Ayako, R.M., Mutiso, J.M., Macharia, J.C., Langoi, D. and Ochola, L. (2021) Concomitant Infection with *Leishmania donovani* and *Plasmodium berghei* Causes Pro-Inflammatory Polarization Resulting in Malaria Exacerbation in BALB/c Mice. *American Journal of Infectious Diseases and Microbiology*, **9**, 71-82. https://doi.org/10.12691/ajidm-9-3-1

[8] Spencer, L.M., Peña-Quintero, A., Canudas, N., Bujosa, I. and Urdaneta, N. (2018) Antimalarial Effect of Two Photo-Excitable Compounds in a Murine Model with *Plasmodium berghei* (Haemosporida: Plasmodiidae). *Revista de Biología Tropical*, **66**, 880-891. https://doi.org/10.15517/rbt.v66i2.33420

[9] Quadros Gomes, A.R., Castro, A.L.G., Ferreira, G.G., Brígido, H.P.C., Varela, E.L.P., Vale, V.V., *et al*. (2024) Impact on Parasitemia, Survival Time and Pro-Inflammatory Immune Response in Mice Infected with *Plasmodium berghei* Treated with *Eleutherine plicata*. *Frontiers in Pharmacology*, **15**, Article 1484934. https://doi.org/10.3389/fphar.2024.1484934

[10] Mutiso, J.M., Macharia, J.C. and Gicheru, M.M. (2012) Immunization with *Leishmania* Vaccine-Alum-BCG and Montanide ISA 720 Adjuvants Induces Low-Grade Type 2 Cytokines and High Levels of Igg2 Subclass Antibodies in the Vervet Monkey (*Chlorocebus aethiops*) Model. *Scandinavian Journal of Immunology*, **76**, 471-477. https://doi.org/10.1111/j.1365-3083.2012.02764.x

[11] Kaye, P. and Scott, P. (2011) Leishmaniasis: Complexity at the Host-Pathogen Inter-

face. *Nature Reviews Microbiology*, **9**, 604-615. https://doi.org/10.1038/nrmicro2608

[12] Lockwood, D. and Moore, E. (2010) Treatment of Visceral Leishmaniasis. *Journal of Global Infectious Diseases*, **2**, 151-158. https://doi.org/10.4103/0974-777x.62883

[13] Salguero, F.J., Garcia-Jimenez, W.L., Lima, I. and Seifert, K. (2018) Histopathological and Immunohistochemical Characterisation of Hepatic Granulomas in *Leishmania donovani*-Infected BALB/c Mice: A Time-Course Study. *Parasites & Vectors*, **11**, Article No. 73. https://doi.org/10.1186/s13071-018-2624-z

[14] Deroost, K., Pham, T., Opdenakker, G. and Van den Steen, P.E. (2015) The Immunological Balance between Host and Parasite in Malaria. *FEMS Microbiology Reviews*, **40**, 208-257. https://doi.org/10.1093/femsre/fuv046

[15] Scaccabarozzi, D., Deroost, K., Corbett, Y., Lays, N., Corsetto, P., Salè, F.O., *et al*. (2018) Differential Induction of Malaria Liver Pathology in Mice Infected with *Plasmodium chabaudi* as or *Plasmodium berghei* NK65. *Malaria Journal*, **17**, Article No. 18. https://doi.org/10.1186/s12936-017-2159-3

[16] Ornellas-Garcia, U., Freire-Antunes, L., Rangel-Ferreira, M., de Sousa, C.H.G., Ribeiro-Almeida, M.L., Daniel-Ribeiro, C.T., *et al*. (2025) Impact of Co-Infection with *Plasmodium berghei* ANKA in *Leishmania* Major-Parasitized Mice on Immune Modulation and Cutaneous Leishmaniasis. *PLOS Neglected Tropical Diseases*, **19**, e0013302. https://doi.org/10.1371/journal.pntd.0013302

[17] Wang, M., Feng, Y., Pang, W., Qi, Z., Zhang, Y., Guo, Y., *et al*. (2014) Parasite Densities Modulate Susceptibility of Mice to Cerebral Malaria during Co-Infection with *Schistosoma japonicum* and *Plasmodium berghei*. *Malaria Journal*, **13**, Article No. 116. https://doi.org/10.1186/1475-2875-13-116

[18] Maspi, N., Abdoli, A. and Ghaffarifar, F. (2016) Pro- and Anti-Inflammatory Cytokines in Cutaneous Leishmaniasis: A Review. *Pathogens and Global Health*, **110**, 247-260. https://doi.org/10.1080/20477724.2016.1232042

[19] Maksoud, S. and El Hokayem, J. (2023) The Cytokine/Chemokine Response in Leishmania/HIV Infection and Co-infection. *Heliyon*, **9**, e15055. https://doi.org/10.1016/j.heliyon.2023.e15055

[20] Murphy, M.L., Wille, U., Villegas, E.N., Hunter, C.A. and Farrell, J.P. (2001) IL-10 Mediates Susceptibility to *Leishmania donovani* Infection. *European Journal of Immunology*, **31**, 2848-2856.

[21] Dayakar, A., Chandrasekaran, S., Kuchipudi, S.V. and Kalangi, S.K. (2019) Cytokines: Key Determinants of Resistance or Disease Progression in Visceral Leishmaniasis: Opportunities for Novel Diagnostics and Immunotherapy. *Frontiers in Immunology*, **10**, Article 670. https://doi.org/10.3389/fimmu.2019.00670

[22] Santana, C.C., de Freitas, L.A.R., Oliveira, G.G.S. and dos-Santos, W.L.C. (2019) Disorganization of Spleen Compartments and Dermatitis in Canine Visceral Leishmaniasis. *Surgical and Experimental Pathology*, **2**, Article No. 14. https://doi.org/10.1186/s42047-019-0040-0

[23] Delahunt, C., Horning, M.P., Wilson, B.K., Proctor, J.L. and Hegg, M.C. (2014) Limitations of Haemozoin-Based Diagnosis of *Plasmodium falciparum* Using Dark-Field Microscopy. *Malaria Journal*, **13**, Article No. 147. https://doi.org/10.1186/1475-2875-13-147

[24] Chadburn, A., Abdul-Nabi, A.M., Teruya, B.S. and Lo, A.A. (2013) Lymphoid Proliferations Associated with Human Immunodeficiency Virus Infection. *Archives of Pathology & Laboratory Medicine*, **137**, 360-370. https://doi.org/10.5858/arpa.2012-0095-ra

[25] Prasad, S., Sheng, W.S., Hu, S., Chauhan, P. and Lokensgard, J.R. (2021) Dysregulated

Microglial Cell Activation and Proliferation Following Repeated Antigen Stimulation. *Frontiers in Cellular Neuroscience*, **15**, Article 686340. https://doi.org/10.3389/fncel.2021.686340

[26] Samant, M., Sahu, U., Pandey, S.C. and Khare, P. (2021) Role of Cytokines in Experimental and Human Visceral Leishmaniasis. *Frontiers in Cellular and Infection Microbiology*, **11**, Article 624009. https://doi.org/10.3389/fcimb.2021.624009

[27] Andoh, N.E. and Gyan, B.A. (2021) The Potential Roles of Glial Cells in the Neuropathogenesis of Cerebral Malaria. *Frontiers in Cellular and Infection Microbiology*, **11**, Article 741370. https://doi.org/10.3389/fcimb.2021.741370

[28] de Oca, M.M., Engwerda, C. and Haque, A. (2013) *Plasmodium berghei* ANKA (PbA) Infection of C57BL/6J Mice: A Model of Severe Malaria. In: Allen, I., Ed., *Mouse Models of Innate Immunity*, Humana Press, 203-213. https://doi.org/10.1007/978-1-62703-481-4_23

[29] Devi, P., Khan, A., Chattopadhyay, P., Mehta, P., Sahni, S., Sharma, S., *et al.* (2021) Co-Infections as Modulators of Disease Outcome: Minor Players or Major Players? *Frontiers in Microbiology*, **12**, Article 664386. https://doi.org/10.3389/fmicb.2021.664386

[30] Mabbott, N.A. (2018) The Influence of Parasite Infections on Host Immunity to Co-Infection with Other Pathogens. *Frontiers in Immunology*, **9**, Article 2579. https://doi.org/10.3389/fimmu.2018.02579